

Hydrophobic, Highly Conductive Ambient-Temperature Molten Salts[†]

Pierre Bonhôte,* Ana-Paula Dias, Nicholas Papageorgiou, Kuppuswamy Kalyanasundaram, and Michael Grätzel*

Institut de chimie physique, Ecole polytechnique fédérale de Lausanne, CH-1015 Lausanne, Switzerland

Received August 15, 1995[⊗]

New, hydrophobic ionic liquids with low melting points (< -30 °C to ambient temperature) have been synthesized and investigated, based on 1,3-dialkyl imidazolium cations and hydrophobic anions. Other imidazolium molten salts with hydrophilic anions and thus water-soluble are also described. The molten salts were characterized by NMR and elemental analysis. Their density, melting point, viscosity, conductivity, refractive index, electrochemical window, thermal stability, and miscibility with water and organic solvents were determined. The influence of the alkyl substituents in 1, 2, 3, and 4(5)-positions on these properties was scrutinized. Viscosities as low as 35 cP (for 1-ethyl-3-methylimidazolium bis((trifluoromethyl)sulfonyl)amide (bis(triflyl)amide) and trifluoroacetate) and conductivities as high as 9.6 mS/cm were obtained. Photophysical probe studies were carried out to establish more precisely the solvent properties of 1-ethyl-3-methylimidazolium bis((trifluoromethyl)sulfonyl)amide). The hydrophobic molten salts are promising solvents for electrochemical, photovoltaic, and synthetic applications.

Introduction

Since the discovery of the first ambient temperature ionic liquid (a *N*-ethylpyridinium bromide–aluminum chloride melt) in 1951,¹ many classes of molten salts have been investigated. For a short review, see Cooper and Sullivan.² The generally highly conductive tetrachloroaluminates and heptachlorodialuminates of cations as 1,3-dialkylimidazolium³ or triazolium,⁴ tetraalkylammonium or phosphonium, and trialkylsulfonium⁵ are water reactive and thus difficult to handle. Molten salts containing low symmetry tetraalkylammonium cation associated to tetraalkylboride,⁶ perchlorate or bromide are either difficult to prepare or weakly conducting. Recently, the remarkable properties of 1-ethyl-3-alkylimidazolium trifluoromethanesulfonates (triflates, TfO⁻) were reported. These ionic liquids exhibit large electrochemical window (> 4 V), good conductivity, and excellent thermal stability.² The acetate of the same cation is reported to melt at -45 °C.⁷

In our search for highly stable solvents for the dye-sensitized nanocrystalline solar cell developed in our group,⁸ we scrutinized

molten salts for their attractive electrochemical and physical properties. Of interest for our photoelectrochemical cell is the minute vapor pressure of the ionic liquids, their good conductivity, and their resistance to oxidation, which can be caused by direct UV-excitation of the dye-supporting semiconductor (TiO₂). Application of molten salts to solar cells will be reported elsewhere. The use of dialkylimidazolium tetrachloroaluminate in photoelectrochemical cells have been reported by Rajeshwar *et al.*,^{3b} but the sensitivity of that material to water precludes its application to solar cells. 1,3-Dialkylimidazolium salts (RR'Im⁺X⁻) appear to be up to now the most stable and conductive ionic liquids. We have therefore synthesized 34 salts based on that type of cation, varying the alkyl substituents in order to establish correlation between chemical structure and physical properties. The 2- and 4(5)-methyl-substituted analogues were also prepared in order to determine whether the viscosity would be affected by the suppression of the C(2)–H···X⁻ or C(4)–H···X⁻ H-bonding which is known to exist with X⁻ = halide, AlCl₄⁻, or CH₃COO⁻.^{7,9–13} Anions were chosen in the perfluorinated series, as strong delocalization of the negative charge weakens the hydrogen bonding with the cation and lowers the viscosity. By lengthening the perfluoroalkyl chain, however, better charge delocalization was found to be largely overcompensated by stronger van der Waals interactions, which led to a viscosity increase.

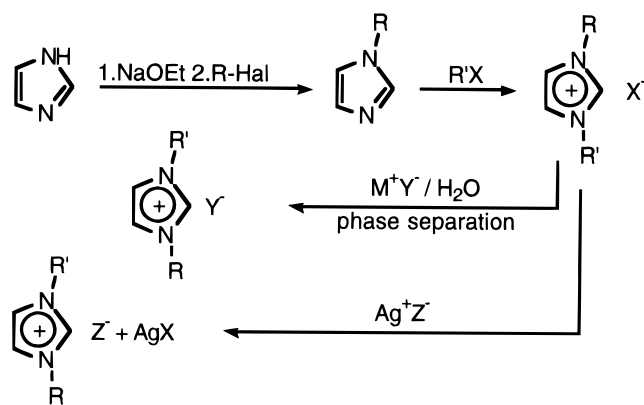
Here, we report for the first time on dialkylimidazolium bis((trifluoromethyl)sulfonyl)amides (bis(triflyl)amides, Tf₂N⁻), which are hydrophobic ionic liquids, saturated by less than 2% of water. Previously, tetraalkylammonium tetraalkylborides had been shown to be hydrophobic.¹⁴ Their low conductivity, potential reactivity, and difficulty of preparation precludes their

[†] Application for a patent on "Hydrophobic molten salts: preparation and application in electrochemistry" was submitted in Switzerland (No. 03 862/94-5) and France (No. 94 15704) on Dec 23, 1994.

[⊗] Abstract published in *Advance ACS Abstracts*, February 1, 1996.

- (1) Hurley, F. H.; Wier, T. P. *J. Electrochem. Soc.* **1951**, *98*, 203.
- (2) Cooper, E. I.; Sullivan, E. J. M. *Proceedings of the 8th International Symposium on Molten Salts*; The Electrochemical Society: Pennington, NJ, 1992; Proceeding Vol. 92-16, pp 386–396 and references cited therein.
- (3) (a) Wilkes, J. S.; Levisky, J. A.; Wilson, R. A.; Hussey, Ch. L. *Inorg. Chem.* **1982**, *21*, 1263–1264. (b) Rajeshwar, K.; DuBow, J. B.; *Proceedings of the 16th Intersociety Energy Conversion Engineering Conference*; SAE: New York, 1981.
- (4) Vestergaard, B.; Bjerrum, N. J.; Petrusina, I.; Hjuler, H. A.; Berg, R. W.; Begtrup, M. *J. Electrochem. Soc.*, **1993**, *140*, 3108–3113.
- (5) Jones, S. D.; Blomgren, G. E.; *J. Electrochem. Soc.* **1973**, *120*, 273–280.
- (6) Gordon, J. E.; Subba Rao, G. N.; *J. Am. Chem. Soc.* **1978**, *100*, 7445–7454.
- (7) (a) Wilkes, J. S.; Zaworotko, M. J. *J. Chem. Soc., Chem. Commun.* **1992**, 965–967. (b) Fuller, J.; Carlin, R. T.; De Long, H. C.; Haworth, D. *Ibid.* **1994**, 299–300.
- (8) (a) Nazeeruddin, M. K.; Kay, A.; Rodicio, J.; Humphrey-Baker, R.; Müller, E.; Liska, P.; Vlachopoulos, N.; Grätzel, M. *J. Am. Chem. Soc.* **1993**, *115*, 6382–6390. (b) O'Regan, B.; Grätzel, M. *Nature (London)* **1991**, *353*, 737–739. (c) Nazeeruddin, M. K.; Liska, P.; Moser, J.; Vlachopoulos, N.; Grätzel, M. *Helv. Chim. Acta*, **1990**, *73*, 1788–1803.

- (9) Avent, A. G.; Chaloner, P. A.; Day, M. P.; Seddon, K. R.; Welton, T. *Proceedings of the 8th International Symposium on Molten Salts*; The Electrochemical Society: Pennington, NJ, 1992; Proceeding Vol. 92–16, pp 98–133.
- (10) Carper, W. R.; Pflug, J. L.; Elias, A. M.; Wilkes, J. S. *J. Phys. Chem.* **1992**, *96*, 3828–3833.
- (11) Abdul-Sada, A. K.; Greenway, A. M.; Hitchcock, P. B.; Mohammed, T. J.; Seddon, K. R.; Zora, J. A. *J. Chem. Soc. Chem. Commun.* **1986**, 1753–1754.
- (12) Dymek, C. J.; Grossie, D. A.; Fratini, A. V.; Adams, W. W. *J. Mol. Struct.* **1989**, *213*, 25–34.
- (13) Dieter, K. M.; Dymek, C. J.; Heimer, N. E.; Rovang, J. W.; Wilkes, J. S. *J. Am. Chem. Soc.*, **1988**, *110*, 2722–2726.

Scheme 1^a

^a R = Me, Et; R' = Me, Et, Bu, *iso*-Bu, CF₃CH₂, CH₃OC₂H₅; X = Br, I, CF₃SO₃, CF₃COO; Z = CF₃COO, C₃F₇COO; M⁺Y⁻ = Li⁺(CF₃SO₂)₂N⁻, K⁺C₄F₉SO₃⁻.

application as useful ionic solvents. 1-Dodecyl-3-ethylimidazolium triflate is also hydrophobic² but the large cation size reduces also in this case the salt character and reduces the conductivity.

Dialkylimidazolium bis(triflyl)amides are easy to prepare, conduct well and are thermally and electrochemically very resistant materials. Their immiscibility with water and solvents of low polarity (ethers, haloalkanes, alkanes) opens interesting perspectives for synthetic and electrochemical applications. Most of our attention was dedicated to the bis(triflyl)amides, as they combine low viscosity and high thermal and electrochemical stability.

Shortly before this paper was submitted, a brief article by Koch *et al.* appeared on the stability of 1,2-dimethyl-3-propylimidazolium bis(triflyl)amide and tris(triflyl)methide toward lithium.¹⁵

Results and Discussion

Synthesis. The syntheses of the dialkylimidazolium molten salts are usually straightforward (Scheme 1). 1-methyl-, 4(5)-methyl-, 2-ethyl-, and 1,2-dimethylimidazole are commercially available. Other 1-alkylimidazole were synthesized by deprotonation of imidazole by sodium or sodium ethanoate followed by alkylation, in ethanol or acetonitrile.¹⁶ Ethylation of 4-methylimidazole takes place preferentially in the 1-position, leading to a ratio between the 1,4- and the 1,5-isomers of about 10 to 1. Alkylation of the 1-alkylimidazole derivatives were carried out in refluxing trichloroethane, a solvent chosen for its stability toward strongly alkylating agents, its moderately high boiling point, and the insolubility of the imidazolium salts in this medium. Alkylation by alkyl triflates proceeded at room temperature, while alkyl bromides needed refluxing. Trifluoroethylation was carried out with a lower yield, using the not very reactive trifluoroethyl triflate obtained from trifluoroethanol and triflic anhydride. Dialkylimidazolium bis-triflylides precipitated as a hydrophobic phase by reacting the corresponding halide or triflate with lithium bis(triflyl)amide in aqueous solution. The same procedure was applied for hydrophobic perfluorobutanesulfonates. EtMeIm⁺NfO⁻ was extracted from the aqueous solution by dichloromethane. Water-soluble acetates (AcO⁻), trifluoroacetates (TA⁻), and heptafluorobutanoates (HB⁻) were prepared from the silver salts and the

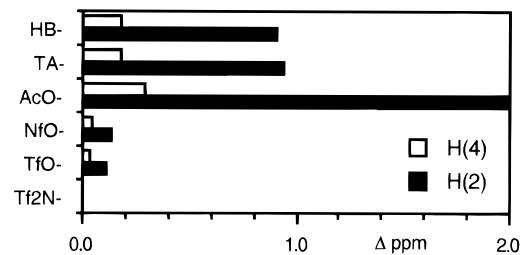


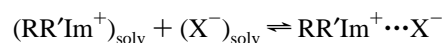
Figure 1. Chemical shift difference between the imidazolium ring protons of various EtMeIm⁺ salts and those of EtMeIm⁺Tf₂N⁻ (interpolated values from Table 1, for a concentration of 0.50 M).

dialkylimidazolium halides. Trifluoroacetates can be prepared on a larger scale via 1-alkylimidazole methylation by methyl trifluoroacetate. This reaction proceeds cleanly, with high yields, somewhat more slowly than with ethyl bromide.

The synthesized salts were submitted to ¹H-NMR and elemental analysis. The salts obtained by direct alkylation sometimes contained less than 1% of the starting 1-alkylimidazole. Bis(triflyl)amides did not contain any detectable impurities. Elemental analyses showed that their lithium and bromide contents lay below the detection limit and thus that the ion exchange process was complete. Water contents after drying, measured by Karl Fisher titration, were 1–2 mM.

¹H-NMR. It has been noticed previously⁹ that the chemical shifts of the imidazolium ring protons are anion- and concentration-dependent. This effect is strong for H–C(2) and weaker for H–C(4) and H–C(5). Two different phenomena have been supposed to affect these chemical shifts: H-bonding and ring stacking. It is well known that the formation of a H-bond causes the proton chemical shift to move to lower field.¹⁷ This relationship is clearly observed for EtMeIm⁺ through our anion series, as presented in Figure 1. At identical concentrations (0.50 M) in acetone-*d*₆, the chemical shifts of the ring protons increase with increasing anion basicity and thus H-bonding ability (Table 1).

The influence of the concentration is more complex. It is expected that a concentration increase will displace the equilibrium



to the right and thus lead to a chemical shift increase. This trend is observed for the H(2) signal only with the most basic anions (TA⁻, HB⁻ and AcO⁻) and at low concentration (Figure 2a). In the case of H(4), it extends over all the concentration range for the same anions (Figure 2b). For the imidazolium salts of the least basic anions (Tf₂N⁻, HB⁻, TfO⁻), however, the H(2) chemical shift *decreases* when the concentration increases. This effect also appears at high concentration for the other anions.

The imidazolium cation, as for any aromatic system, generates two magnetically shielding cones above and below its molecular plane, classically seen as caused by an electronic current circulating around the π-orbitals, on both sides of the aromatic ring. A proton penetrating into these cones will have an NMR signal moving to higher field. Following Welton *et al.*⁹ it is supposed that with concentration increase, the imidazolium cations progressively form ions pairs with the anions, which stack as the neutral aromatic systems do. This stacking has

(14) Ford, W. T.; Hauri, R. J.; Hart, D. J. *J. Org. Chem.* **1973**, *38*, 3916–3918.

(15) Koch, V. R.; Nanjundiah, C.; Battista Appetecchi, G.; Scrosati, B. *J. Electrochem. Soc.* **1995**, *142*, L116–L118.

(16) Begtrup, M.; Larsen, P. *Acta Chem. Scand.* **1990**, *40*, 1050–1057.

(17) a) Hesse, M.; Meier, H.; Zeeh, B.: *Spektroskopische Methoden in der organischen Chemie*, 2nd ed.; Thieme Verlag: Stuttgart, Germany, 1984. (b) Akitt, J. W. *NMR and Chemistry: an introduction to the Fourier Transform-Multinuclear Era*, 2nd ed.; Chapman and Hall: London, 1983.

Table 1. $^1\text{H-NMR}$ Chemical Shifts (δ/ppm Relative to TMS) of MeEtIm^+ Salts as a Function of the Concentration, in Acetone- d_6

a. Triflate (TfO^-)						
[salt]/M	H(2)	H(4)	H(5)	CH_3	CH_2	CH_2CH_3
0.028	9.112	7.791	7.721	4.413	4.065	1.573
0.070	9.107	7.785	7.713	4.404	4.055	1.567
0.188	9.101	7.782	7.707	4.395	4.046	1.562
0.307	9.093	7.780	7.705	4.389	4.040	1.559
0.543	9.077	7.776	7.699	4.379	4.032	1.553
0.988	9.056	7.775	7.695	4.370	4.025	1.549
1.629	9.032	7.774	7.692	4.362	4.020	1.548
1.797	9.028	7.775	7.692	4.360	4.019	1.548
b. Nonaflate (NfO^-)						
[salt]/M	H(2)	H(4)	H(5)	CH_3	CH_2	CH_2CH_3
0.033	9.110	7.795	7.724	4.413	4.065	1.571
0.070	9.111	7.792	7.720	4.408	4.059	1.568
0.139	9.106	7.787	7.714	4.400	4.051	1.563
0.237	9.103	7.788	7.712	4.396	4.047	1.561
0.416	9.095	7.787	7.709	4.390	4.041	1.557
0.718	9.084	7.789	7.708	4.384	4.036	1.554
1.119	9.073	7.793	7.709	4.380	4.035	1.554
1.777	9.060	7.796	7.709	4.377	4.035	1.554
c. Bis(triflyl)amide (Tf_2N^-)						
[salt]/M	H(2)	H(4)	H(5)	CH_3	CH_2	CH_2CH_3
0.020	9.073	7.804	7.739	4.430	4.085	1.564
0.048	9.056	7.793	7.722	4.422	4.077	1.580
0.112	9.034	7.780	7.710	4.414	4.067	1.577
0.225	9.005	7.763	7.691	4.401	4.056	1.572
0.430	8.973	7.744	7.672	4.391	4.045	1.571
0.770	8.925	7.715	7.642	4.372	4.028	1.564
1.209	8.873	7.686	7.612	4.357	4.015	1.563
1.800	8.811	7.643	7.569	4.334	3.995	1.559
d. Acetate (AcO^-)						
[salt]/M	H(2)	H(4)	H(5)	CH_3	CH_2	CH_2CH_3
0.028	10.843	7.743	7.672	4.425	4.069	1.544
0.038	10.985	7.821	7.742	4.427	4.071	1.535
0.104	11.013	7.807	7.728	4.426	4.070	1.535
0.314	11.003	7.945	7.858	4.430	4.074	1.522
0.517	10.959	8.037	7.943	4.430	4.076	1.511
0.839	10.938	8.142	8.038	4.433	4.081	1.502
1.239	10.981	8.261	8.140	4.435	4.088	1.495
1.815	10.921	8.336	8.205	4.440	4.096	1.490
e. Trifluoroacetate (TA^-)						
[salt]/M	H(2)	H(4)	H(5)	CH_3	CH_2	CH_2CH_3
0.026	9.827	7.807	7.733	4.417	4.066	1.557
0.077	9.902	7.829	7.750	4.414	4.062	1.551
0.183	9.913	7.858	7.776	4.412	4.060	1.546
0.447	9.910	7.908	7.818	4.410	4.059	1.539
0.996	9.888	7.967	7.870	4.408	4.060	1.533
1.802	9.868	8.025	7.919	4.411	4.069	1.533
f. Heptafluorobutanoate (HB^-)						
[salt]/M	H(2)	H(4)	H(5)	CH_3	CH_2	CH_2CH_3
0.020	9.754	7.805	7.731	4.416	4.065	1.557
0.061	9.834	7.822	7.745	4.413	4.061	1.552
0.122	9.858	7.846	7.764	4.413	4.060	1.547
0.242	9.873	7.876	7.791	4.412	4.059	1.544
0.473	9.873	7.917	7.825	4.411	4.059	1.537
0.860	9.866	7.965	7.866	4.413	4.062	1.534
1.341	9.862	8.013	7.906	4.418	4.069	1.535
1.804	9.859	8.055	7.941	4.424	4.079	1.537

been observed by X-ray crystallography in the solid state, by Welton *et al.*¹⁸ Thus, the chemical shift displacement with concentration can be analyzed in terms of two effects: H-bonding leading to higher shifts and ring stacking leading to

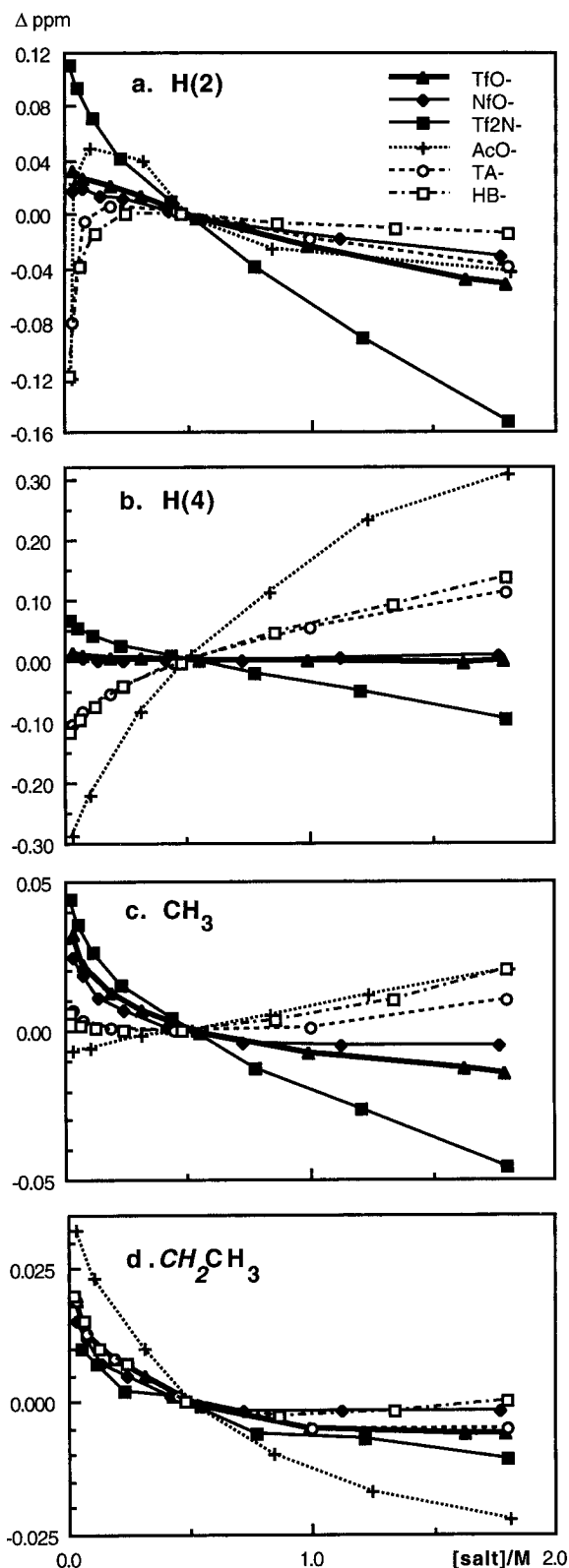


Figure 2. $^1\text{H-NMR}$ chemical shifts (δ/ppm relative to TMS) of various EtMeIm^+ salts as a function of the concentration, in deuterated acetone. The displacement of the shift is given relative to the value at 0.500 M (interpolated).

lower shifts. The extreme case is that of the CH_3 protons of the ethyl group. Being unable to H-bond, they are only affected by ring stacking (Figure 2d). For the other protons, both effects can be observed, depending on the nature of the anion and on its concentration.

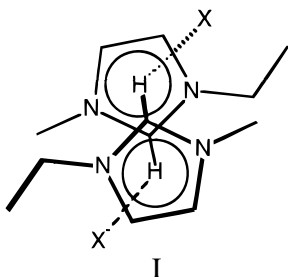
With the most basic anions, the influence of concentration is in part or completely opposite for H(2) and H(4). This can be

Table 2. Melting Points (°C) of the Imidazolium Salts

Im ⁺	TfO ⁻	NfO ⁻	Tf ₂ N ⁻	TA ⁻	HB ⁻
3-Me					
1-Me	39		22	52	
1-Et	-9	28	-3	-14	<i>a</i>
1-Bu	16	20	-4	<i>a</i>	<i>a</i>
1- <i>i</i> -Bu			<i>a</i>		
1-MeOEt	27		<i>a</i>		
1-CF ₃ CH ₂	45		<i>a</i>		
3-Et					
1-Et	23		14	<i>a</i>	
1-Bu	2	21	<i>a</i>	<i>a</i>	
1-Et					
2,3-Me ₂	109		20	59	
2-Et-3-Me	113		28		
1-Et-5-Me					
3-Me	6		-3		
3-Et	35		-22		

^a Could not be crystallized. Turned into a glass between -30 and -50 °C.

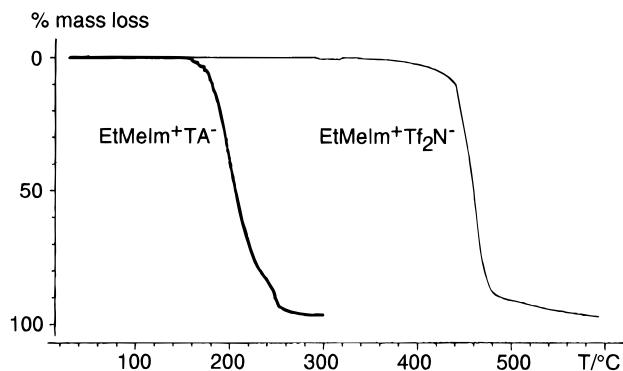
rationalized based on the top-to-bottom structure proposed by Welton (structure I). It can be assumed that the stacking will



take place the closest to that model for the most tightly bound ion-pairs, which means for the most basic anions. With a concentration increase, the H(2) entering the shielding cone of the neighboring imidazolium moves to lower shifts while the H(4) and H(5), pointing outside, remain only influenced by H-bonding strengthening. At the other extreme, Tf₂N⁻, the least basic anion, appears unable to H-bond, as indicated by the hydrophobicity of its imidazolium salts. Ion-pairing probably proceeds at random, without preferential orientation, and aggregation can occur with H(2) as well as H(4) or H(5) in the shielding cone of the neighboring imidazolium ring. Referring to the X-ray structure of EtMeIm⁺PF₆⁻,^{7b} one can in fact assume that there is no proper stacking in dialkylimidazolium salts of non-hydrogen-bonding anions, but only randomized aggregation.

Melting Points (Table 2). The melting points are difficult to correlate with the chemical composition of the salts. 1,3-Dialkylimidazolium bis(triflyl)amides, trifluoroacetates, and heptafluorobutanoates are generally liquid up to -30 to -50 °C and become increasingly viscous, turning finally into glasses. EtMeIm⁺AcO⁻ behaves identically. Triflates and nonaflates often melt close to room temperature, except 1-Et-3-MeIm⁺TfO⁻, for which the melting point corresponds to that reported previously.² The effect of cation symmetry is obvious: Me₂Im⁺ and Et₂Im⁺ salts present higher melting points than the salts with unsymmetrical cations.

It appears from the examination of the anion series that there are no obvious correlations between H-bonding ability and melting point. A strongly H-bonding anion with weak charge delocalization (AcO⁻) forms an EtMeIm⁺ salt of very low glass transition temperature but an anion unable to H-bond and bearing a strongly delocalized charge (Tf₂N⁻) also does. It was expected at first that suppressing the C(2)-H...X⁻ H-bond by alkyl substitution would lower the melting point. The opposite

**Figure 3.** Thermogravimmetry in air of EtMeIm⁺Tf₂N⁻ and EtMeIm⁺TA⁻.

was observed; C(2) methylation or ethylation increases the melting point by 50 to 120 °C and makes the vitrous solids quite crystalline. Methylation in the 5-position also augments the melting point, albeit to a lesser extent.

The influence of H-bonding and charge delocalization can only be understood for structurally similar anions such as TfO⁻ and Tf₂N⁻. The lower melting point of the latter is probably related to its inability to H-bond and to its better charge delocalization. This hypothesis is supported by the large difference between the melting point of EtMeIm⁺TfO⁻ and CF₃CH₂MeIm⁺TfO⁻, the trifluoroethylated imidazolium being more susceptible to H-bonding due to the CF₃CH₂ electron-withdrawing effect on the Im⁺ ring (see NMR). No such difference is noticed for the Tf₂N⁻ analogues. The effect of the cation symmetry on the other hand, appears for both Tf₂N⁻ and TfO⁻ salts.

The van der Waals interactions have only a slight influence on the melting point, obvious only when comparing triflates and nonaflates of the same cations. Alkyl chain lengthening on the cation can lead to opposite effects.

Thermal Stability. The thermal stabilities of EtMeIm⁺TfO⁻, Tf₂N⁻, and TA⁻ in air as well as under nitrogen were determined on a Mettler thermogravimetric balance at a heating rate of 10 °C/min. The two former were stable up to 400 °C and decomposed rapidly between 440 and 480 °C at a constant rate, both in air and under N₂. The latter was much less stable and started to decompose at 150 °C in air or N₂, the process lasting up to 250 °C, in a more complex mode as illustrated in Figure 3.

Miscibility with Other Liquids. All the investigated molten salts are miscible with liquids of medium and high dielectric constant (ϵ): low alcohols and ketones, dichloromethane ($\epsilon = 8.93$), and THF ($\epsilon = 7.58$). They are immiscible with alkanes, dioxane ($\epsilon = 2.01$), toluene ($\epsilon = 2.38$), and diethyl ether ($\epsilon = 4.33$). Ethyl acetate ($\epsilon = 6.02$) appears to constitute the borderline. EtMeIm⁺TfO⁻, NfO⁻, and Tf₂N⁻ are miscible with this solvent, while TA⁻ and HB⁻ are slightly soluble. Alkyl chain lengthening increases the solubility: BuMeIm⁺TA⁻ and BuMeIm⁺HB⁻ are miscible with ethyl acetate.

Triflates, trifluoroacetates, and heptafluorobutyrate are miscible with water (Table 3) for all the dialkylimidazolium cations investigated (up to BuEtIm⁺). Nonaflate miscibility is limited early by alkyl chain lengthening. All the bis(triflyl)amides are immiscible with water, reflecting the absence of H-bonding ability of the anion. Alkyl chain length has no strong influence in this case. The saturating water content is the same for EtMeIm⁺Tf₂N⁻ and for BuMeIm⁺Tf₂N⁻. It is slightly higher for the MeOC₂H₄MeIm⁺ and CF₃CH₂MeIm⁺ salts due to increased H-bonding possibilities with the cation, caused by the presence of an oxygen atom in the side chain for the former

Table 3. Water Content at Saturation in Mass %, at 20 °C, of the Imidazolium Salts Which Are Liquids or Supercooled Liquids at That Temperature^a

Im ⁺	TfO ⁻	NfO ⁻	Tf ₂ N ⁻	TA ⁻	HB ⁻
3-Me					
1-Me	s		2.5	s	
1-Et	s	s	1.4	s	
1-Bu	s	17.5	1.4	s	s
1- <i>i</i> -Bu			1.5		
1-MeOEt	s		3.0		
1-CF ₃ CH ₂	s		2.5		
3-Et					
1-Et	s		2.0	s	
1-Bu		8.9	1.3	s	
1-Et-2-Me					
3-Me			1.8		
1-Et-5-Me					
3-Me	s		2.2		
3-Et	s		1.7		

^a s: water soluble. Determination by Karl-Fisher titration; estimated error: ± 7%.

Table 4. Dynamic Viscosity at 20 °C (cP (0.01 g cm⁻¹ s⁻¹)) of the Imidazolium Salts Which Are Liquids or Supercooled Liquids at That Temperature^a

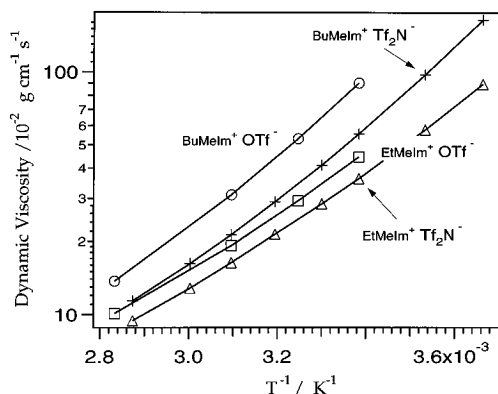
Im ⁺	TfO ⁻	NfO ⁻	Tf ₂ N ⁻	TA ⁻	HB ⁻	AcO ⁻
3-Me						
1-Me			44			
1-Et	45		34	35	105	162
1-Bu	90	373	52	73	182	
1- <i>i</i> -Bu			83			
1-MeOEt	74		54			
1-CF ₃ CH ₂			248			
3-Et						
1-Et	53		35	43		
1-Bu		323	48	89		
1-Et-2-Me						
3-Me			88			
1-Et-5-Me						
3-Me	51		37			
3-Et			36			

^a Estimated error: ± 5%.

and to increased Im⁺-ring charge for the latter. The solubility of EtMe⁺Tf₂N⁻ in water is 1.8%, as determined by removing the water from a 10.00 mL saturated solution.

Viscosity (Table 4). The viscosities of the liquid salts appear to be governed essentially by van der Waals interactions and H-bonding. From TfO⁻ to NfO⁻ and from TA⁻ to HB⁻, the increase of the van der Waals attraction obviously dominates over the H-bonding decrease and better charge delocalization. From TfO⁻ to Tf₂N⁻, however, almost complete H-bonding suppression slightly dominates over the van der Waals attraction increase. Comparing TA⁻ and AcO⁻ reveals the opposite trend; much stronger H-bonding overcompensates for smaller anion weight. TA⁻ and Tf₂N⁻ salts present the lowest viscosities as they combine minimal anion weight with moderate basicity for the former and minimal basicity with moderate anion weight for the latter.

The cation structure also influences the salt viscosity. The minimal values are obtained for EtMeIm⁺ salts, which combine sufficient side chain mobility and low molecular weight. Alkyl chain lengthening or fluorination makes the salt more viscous, due to increased van der Waals interactions. Alkyl chain ramification (from butyl to isobutyl) has the same effect, due to reduced rotation freedom. It was expected that replacing a butyl substituent by a methoxyethyl would decrease the viscosity by increasing the chain mobility but no such effect can be observed. Methylation at C(2), but not at C(4), increases the

**Figure 4.** Plot of dynamic viscosity (η , estimated error: $\pm 5\%$) of some ambient temperature molten salts as function of reciprocal absolute temperature (T^{-1}).

viscosity as it does for the melting point. This fact is striking as, again, H-bonding suppression was expected to reduce the viscosity.

For unassociated liquid electrolytes, the empirical equation giving the temperature dependence of the dynamic viscosity is also applicable in ionic liquid systems:¹⁹

$$\eta = Ae^{\epsilon/RT} \quad (1)$$

where ϵ is the activation energy for viscous flow. Following eq 1, the logarithmic plot of η vs T^{-1} should give a straight line, unless near the melting point where ion association into aggregates begins. Figure 4 shows that the plots are not perfectly linear, as previously noticed.² The obtained ϵ value is 29 kJ/mol for MeBuIm⁺TfO⁻ and 21 kJ/mol for MeEtIm⁺Tf₂N⁻.

Conductivity. The conductivity of a liquid salt can be described by eq 2, where C_a' , C_c' , u_a , u_c are the anion and cation

$$\sigma = F \sum C_i' u_i = F(C_a' u_a + C_c' u_c) \quad (2)$$

concentrations and mobilities in the melt. It follows that $C_a' = C_c' = yC$, where $C = d/FW$ and $0 < y < 1$ is the degree of dissociation. Therefore

$$\sigma = yFC(u_a + u_c) \quad (3)$$

A more accurate modified form of the Stokes–Einstein relation²¹ correlates ionic transport to viscosity of the medium even in molten salts:¹⁹

$$D_a = RT/(6\pi N_A \zeta_a r_a \eta) \quad D_c = RT/(6\pi N_A \zeta_c r_c \eta) \quad (4)$$

where ζ_a and ζ_c are the anion and cation microviscosity factors respectively.

Combination with

$$D_a = u_a RT/F \quad D_c = u_c RT/F \quad (5)$$

derives the relation between specific conductivity and anion,

(19) Bockris, J. O'M.; Reddy, A. K. *Modern Electrochemistry*; Plenum Press: New York, 1970; Vol. 1, pp 547–553.

(20) Kissinger, P. T.; Heineman, W. R. *Laboratory Techniques in Electroanalytical Chemistry*; Bard, A., Ed.; Dekker Inc.: New-York, 1984.

(21) Koryta, J.; Dvorak, J.; Kavan, L. *Principles of Electrochemistry*; John Wiley & Sons: Chichester, England, 1993; pp 120–124.

Table 5. Specific Conductivity at 20 °C (mS cm⁻¹) of the Imidazolium Salts Which Are Liquids or Supercooled Liquids at That Temperature^a

Im ⁺	TfO ⁻	NfO ⁻	Tf ₂ N ⁻	TA ⁻	HB ⁻	AcO ⁻
3-Me						
1-Me			8.4			
1-Et	8.6		8.8	9.6	2.7	2.8
1-Bu	3.7	0.45	3.9	3.2	1.0	
1- <i>i</i> -Bu			2.6			
1-MeOEt	3.6		4.2			
1-CF ₃ CH ₂			0.98			
3-Et						
1-Et	7.5		8.5	7.4		
1-Bu		0.53	4.1	2.5		
1-Et-2-Me						
3-Me						
1-Et-5-Me						
3-Me	6.4		6.6			
3-Et			6.2			

^a Estimated error: ± 5%.**Table 6.** Density at 22 °C (or at the Indicated Temperature) (g cm⁻³) of the Imidazolium Salts Which Are Liquids or Supercooled Liquids at that Temperature

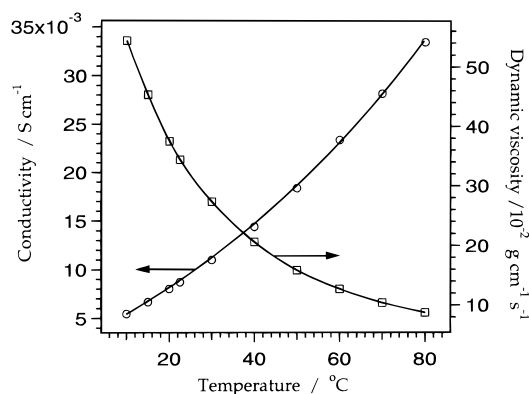
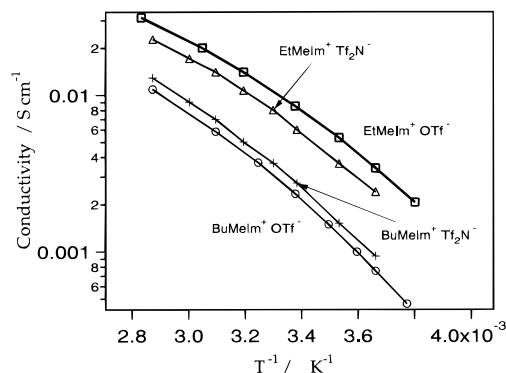
Im ⁺	TfO ⁻	NfO ⁻	Tf ₂ N ⁻	TA ⁻	HB ⁻
3-Me					
1-Me			1.559		
1-Et	1.390		1.520	1.285	1.450
1-Bu	1.290 ²⁰	1.473 ¹⁸	1.429 ¹⁹	1.209 ²¹	1.333
1- <i>i</i> -Bu			1.428 ²⁰		
1-MeOC ₂ H ₄	1.364		1.496		
1-CF ₃ CH ₂			1.656 ²⁰		
3-Et					
1-Et	1.330		1.452 ²¹	1.250	
1-Bu		1.427 ¹⁸	1.404 ¹⁹	1.183 ²³	
1-Et-2-Me					
3-Me					
1-Et-5-Me					
3-Me	1.334 ²⁰		1.470		
3-Et			1.432 ²³		

cation hydrodynamic radii.

$$\sigma = yF^2d/(6\pi N_A FW\eta) [(\zeta_a r_a)^{-1} + (\zeta_c r_c)^{-1}] \quad (6)$$

This includes the “correction” factor ζ taking into account the specific interactions between the mobile ions in the melt. The conductivities of the liquid salts can thus, to a reasonable degree of approximation, be related to their viscosities (η), formula weight (FW), and densities (d) and to the radii of their ions (r_a and r_c), following eq 6. Qualitatively, the relationship between conductivity and other physical parameters expressed by eq 6 appears to be verified. Besides the obvious influence of the viscosity, the effect of ion size and weight must be stressed. EtMeIm⁺TA⁻ for instance, is more conducting than the corresponding Tf₂N⁻ salt as, with the same viscosity and in spite of a lower density, it combines the advantages of a lower FW and a smaller anion. Also, while having similar viscosity and density, EtMeIm⁺TfO⁻ and BuEtIm⁺Tf₂N⁻ have conductivities differing by a factor of 2, for the same reason. In the search for highly conducting ionic liquids, one must not focus on viscosity only, but keep in mind the importance of ion size.

Electrochemical Window. The investigated ionic liquids display a large electrochemical window (Figure 7). The oxidation, which presumably concerns the anion, starts at the lowest potential for trifluoroacetate, indicating a decarboxylation reaction. Triflates and bis(triflyl)amides are not oxidized before 2 V vs I⁻/I₃⁻. On the reductive side, a difference between cations can be observed. It is believed that reduction of 1,3-

**Figure 5.** Specific conductivity (σ) and dynamic viscosity (η) of MeEtIm⁺Tf₂N⁻ as a function of temperature (°C). Estimated error: ±5%.**Figure 6.** Specific conductivity (σ , estimated error: ± 5%) of some ionic liquids as a function of the reciprocal absolute temperature (T^{-1}).**Table 7.** Refractive Indexes at 20°C of the Imidazolium Salts Which Are Liquids or Supercooled Liquids at That Temperature

Im ⁺	TfO ⁻	NfO ⁻	Tf ₂ N ⁻	TA ⁻	HB ⁻
3-Me					
1-Me			1.4220		
1-Et	1.4332		1.4231	1.4405	
1-Bu	1.4380	1.4052	1.4271	1.4487	1.4142
1- <i>i</i> -Bu			1.4289		
1-MeOEt	1.4428		1.4293		
1-CF ₃ CH ₂			1.4090		
3-Et					
1-Et	1.4367		1.4260	1.4431	
1-Bu		1.4025	1.4285	1.4441	
1-Et-2-Me					
3-Me					
1-Et-5-Me					
3-Me	1.4400		1.4275		
3-Et			1.4300		

dialkylimidazolium is related to the H(2) acidity. Deprotonation of imidazolium at C(2) is feasible with strong bases (*t*-BuO⁻) and leads to quite stable carbenes.²² Deprotonation of 2-methylated homologues is more difficult and requires stronger bases (*t*-BuLi), leading to an enediamine with strong ylide character.²³ The more negative reduction potentials of 2-methylimidazoliums observed on Figure 7 is probably linked to their weaker acidity.

Photophysical Probe Studies. Photophysical studies are versatile to probe the microenvironments of solvents and organized structures. Their extremely high sensitivities allow studies conducted at very low probe concentration ($\leq 10^{-5}$ M)

- (22) (a) Arduengo, A. J.; Harlow, R. L.; Kline, M. *J. Am. Chem. Soc.* **1991**, *113*, 361. (b) Arduengo, A. J.; Dias, H. V. R.; Harlow, R. L.; Kline, M. *Ibid.* **1992**, *114*, 5530.
 (23) Kuhn, H.; Bohnen, H.; Kreutzberg, J.; Bläser, D.; Boese, R. *J. Chem. Soc. Chem. Commun.* **1993**, 1136–1137.

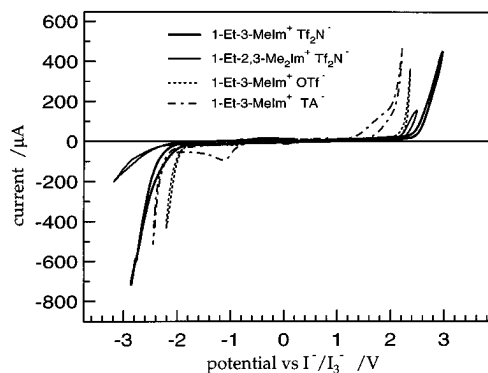


Figure 7. Cyclic voltammograms for a stationary Pt electrode (0.78 mm²) in various ionic liquids at 23 °C. Sweep rate: 50mV/s. The I⁻/I₃⁻ couple has a measured potential of -0.195 V vs ferrocene/ferrocenium in EtMeIm⁺Tf₂N⁻. The reduction current observed in the vicinity of -1.0 V in EtMeIm⁺TA⁻ appears to result from the reduction of dissolved H₂O. Effective drying of this salt could not be performed because of the low decomposition temperature (see Figure 3).

and thus examination of the host environment in nearly unperturbed state. A large number of fluorescence probes are available to determine the polarity, microviscosity, state of protonation, etc. Facile observation of room temperature phosphorescence from solubilized molecules in organized media such as micelles and hosts such as cyclodextrins has led to recent developments of a number of phosphorescent probes.²⁴ Hereafter we describe some of our results on fluorescence and phosphorescence probe studies of EtMeIm⁺Tf₂N⁻. The molten salt is optically transparent at $\lambda \geq 300$ nm, allowing direct excitation of dissolved probe molecules in the UV region.

a. Fluorescence Studies Using Pyrenecarboxaldehyde (Py-CHO). Py-CHO has two types of low-lying excited states, (n, π^*) and (π, π^*), both of which show emission in fluid solution at room temperature. In nonpolar solvents such as *n*-hexane, the emission is highly structured and weak arising from the (π, π^*) excited state. The upper-lying (n, π^*) excited state is solvent-sensitive and can undergo relaxation in polar solvents. When the dielectric constant (ϵ) of the solvent exceeds ca. 10, the emission consists of broad, moderately intense fluorescence around 400–500 nm coming exclusively from the (n, π^*) excited state. The emission maximum red-shifts linearly with increasing ϵ , at $\epsilon > 10$; for instance: 1-hexanol ($\epsilon = 13.5$), 440 nm; *n*-PrOH ($\epsilon = 20.8$), 443 nm; and CH₃OH ($\epsilon = 33.0$), 450 nm. The fluorescence quantum yield (ϕ) also increases with ϵ . In pure methanol, $\phi = 0.15$ when in methanol–water 1:1, $\phi = 0.69$. For this reason, Py-CHO has been used as a probe of solvent polarity in various microheterogeneous systems.²⁵

The emission spectrum of Py-CHO in EtMeIm⁺Tf₂N⁻ at 20 °C shows a maximum at 431 nm, typical from a solvent of very low ϵ (below 10). The observation of several well-resolved maxima in the absorption spectrum of Py-CHO in EtMeIm⁺Tf₂N⁻ is also consistent with very low polarity of the medium. The lowest energy band appears well resolved and intense at 392 nm. In polar solvents such as methanol, the absorption spectrum becomes diffuse with the lowest energy band appearing as a weak shoulder. Py-CHO dissolved in EtMeIm⁺Tf₂N⁻ shows

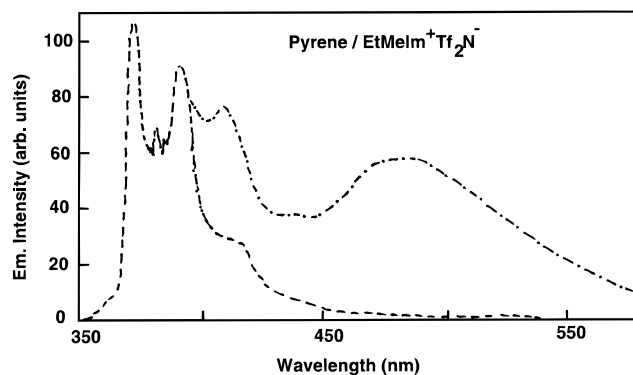


Figure 8. Pyrene fluorescence in degassed EtMeIm⁺Tf₂N⁻; excitation wavelength: 345 nm. Trace A: [pyrene] $\leq 10^{-5}$ M. Trace B: broad excimer emission at [pyrene] = 5×10^{-4} M.

absorption (and the excitation for the emission) spectral features very similar to those observed in hexane with distinct maxima at 394, 374, 362 nm.

By addition of methanol to EtMeIm⁺Tf₂N⁻, the emission maximum red-shifts and gains intensity: at 10% (w/w) methanol, the maximum is at 440 nm, corresponding to $\epsilon = 13$. The maximum is sensitive enough to show red shift even upon addition of 1% methanol.

b. Fluorescence Probe Studies Using Pyrene. Pyrene is a highly fluorescent aromatic molecule showing interesting properties that find applications in different domains. We consider here two specific cases, viz., the Ham effect on the monomer fluorescence and the dynamics of excimer formation. The monomer fluorescence shows several bands corresponding to different vibrational transitions, some of which are very solvent-sensitive. While the third band (0–737 cm⁻¹ transition) is medium-insensitive, the 0–0 band (located at ca. 373 nm) gains considerable intensity in polar solvents. The phenomenon has been widely studied and is known as the “Ham effect”. The ratio of the third to the first band (“the 3/1 ratio”) is a good qualitative measure of the environmental polarity and finds extensive applications in fluorescence probe studies of microheterogeneous systems.²⁶ This ratio is 1.65 in *n*-hexane and decreases with increasing solvent “polarity” (0.98 in *n*-BuOH, 0.75 in CH₃OH and 0.54 in CH₃CN).

Figure 8 shows a representative monomer fluorescence spectrum of pyrene in neat EtMeIm⁺Tf₂N⁻. The measured (3/1) ratio of 0.85 ± 0.05 is close to that of ethanol.

The emission decays exponentially with a lifetime of 300 ns in degassed EtMeIm⁺Tf₂N⁻. Quenching of fluorescence by dissolved oxygen is very efficient. In aerated solutions, the measured lifetime is 145 ns. An estimate for the oxygen solubility in aerated solution can be made using these two measured emission lifetimes and a calculated rate constant based on the Smolouchowski/Stokes–Einstein equations. For a viscosity of 36 cP (Table 4), one obtains $k_{\text{diff}} = 1.8 \times 10^9$ M⁻¹s⁻¹ and this in turn gives the oxygen solubility of $\approx 2 \times 10^{-3}$ M in nondegassed EtMeIm⁺Tf₂N⁻, close to that of organic solvents like benzene (1.9 mM) or ethanol (2.07 mM). Quenching studies in oxygen-purged solutions indicate the saturation solubility to be $\approx 6 \times 10^{-3}$ M.

A broad, structureless emission (with a maximum around 480 nm) attributable to well-known “excimers” can be readily observed in EtMeIm⁺Tf₂N⁻ solutions with [pyrene] $\geq 10^{-5}$ M.

(24) (a) Kalyanasundaram K. *Photochemistry in Organized and Constrained Media*; Ramamurthy V., Ed.; VCH Publishers: New York, 1991; Chapter 2. (b) Kalyanasundaram, K. *Photochemistry in Microheterogeneous Systems*; Academic Press: New York, 1987.
(25) (a) Kalyanasundaram K.; Thomas, J. K. *J. Phys. Chem.* **1977**, *81*, 2176–2180. (b) Dederens, J. C.; Oosemans, L. C.; DeSchryver, F. C.; van Dormael, A. *Photochem. Photobiol.* **1979**, *30*, 443–447. (c) Kumar, C. V.; Chattopadhyay, S. K.; Das, P. K. *Ibid.* **1983**, *38*, 141–152.

(26) (a) Kalyanasundaram K.; Thomas, J. K. *J. Am. Chem. Soc.* **1977**, *99*, 2039–2044. (b) Nakajima, A.; *Spectrochim. Acta* **1974**, *30A*, 360–364. Dong, D. C.; Winnik, M. A., *Photochem. Photobiol.* **1982**, *35*, 17–21. Lianos P.; Georghiou, S. *Ibid.* **1979**, *30*, 355–362.

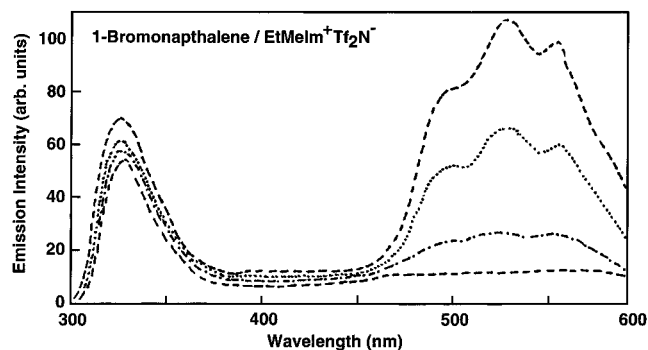


Figure 9. Emission spectra of 1-bromonaphthalene in $\text{EtMeIm}^+\text{Tf}_2\text{N}^-$: aerated (trace A), partially deaerated (traces B and C) and fully degassed (trace D) solution. The high energy emission ($\lambda_{\text{max}} = 331$ nm) corresponds to fluorescence, and the low energy emission ($\lambda_{\text{max}} = 556, 530,$ and 498 nm) corresponds to room temperature phosphorescence. Excitation wavelength: 280 nm.

c. Phosphorescence Studies Using Bromonaphthalene. To study excited state bimolecular processes on longer time scales ($\geq \mu\text{s}$) in $\text{EtMeIm}^+\text{Tf}_2\text{N}^-$, we examined possible “phosphorescence” of 1-bromonaphthalene. It has been shown earlier²⁷ that, due to a combination of factors such as internal heavy atom effect and high microviscosity in the microenvironment, molecules like 1-BrNaph show distinct phosphorescence at room temperature in organized host media like ionic micelles and cyclodextrins. Examination of the emission of 1-BrNaph in $\text{EtMeIm}^+\text{Tf}_2\text{N}^-$ showed only typical fluorescence (with a maximum at 331 nm) in aerated solutions. Purging the solution with Ar leads to appearance of a distinct emission characteristic of “phosphorescence”, as shown in Figure 9. Letting oxygen in leads to disappearance of the phosphorescence. The oxygen effect on the quenching of the fluorescence is rather small due to very short lifetime of the fluorescence.

Observation of room temperature phosphorescence (RTP) in fluid solution of $\text{EtMeIm}^+\text{Tf}_2\text{N}^-$ is remarkable. It raises fundamental questions about what controls the room temperature phosphorescence (RTP) of aromatic molecules. The probe molecule does not show any phosphorescence in degassed solutions of neat, low viscosity solvents such as cyclohexane or methanol. The following are some of the mechanisms widely invoked to explain the absence of RTP: efficient quenching of triplets via triplet-triplet and triplet-ground state annihilation, quenching by molecular oxygen, and medium effects (viscosity). The ready observation of RTP in organized media or hosts (micelles, cyclodextrins) is due to near-elimination of bimolecular quenching pathways. Increased viscosity in the local microenvironment certainly play a role though this effect is difficult to quantify. The ready observation of phosphorescence in low temperature glasses arises both from combined effects of temperature and from viscosity changes. Studies are underway to correlate RTP with viscosity, through a series of molten salts.

Conclusions. Ionic liquids based on imidazolium cation and six different anions have been studied. Low melting point, low viscosity, and high conductivity, which are the desired properties for an ionic liquid, appear to depend on the following requirements. Both the anion and the cation must be small and bear a well-delocalized charge; symmetry of the imidazolium cation is to be avoided for low melting point; the imidazolium C(2)

must not be alkylated. If the two former principles are quite obvious, the reason for the latter remains unclear.

Bis(triflyl)amides display exceptional properties, combining hydrophobicity, high thermal and electrochemical stability, low viscosity, high conductivity, and a very low melting point. They are easier and much cheaper to prepare than the previously known triflates and can be readily obtained in very pure state. NMR and water solubility show that Tf_2N^- behaves as a non-hydrogen-bonding anion. In spite of their apparent low dielectric constant that can be attributed to ion-pairing in the pure state, these ionic liquids are able to solubilize salts. This characteristic and their immiscibility with water and nonpolar liquids opens exciting perspectives of use for imidazolium bis-(triflyl)amides as solvent for synthetic and electrochemical applications. They meet the requirements exposed in the introduction for a stable solvent to be used in photoelectrochemical cells.

Exploratory studies using aromatic hydrocarbons as probes indicate intriguing effects of these new solvents on their luminescence properties in particular the occurrence of room temperature phosphorescence.

Experimental Section

Methods. Water contents were determined by Karl Fisher coulometry using a Metrohm 684 KF coulometer. Melting points were determined visually on 1 g samples, as the middle of an about 3 °C melting range, with an Ebro TFX 392 digital thermometer (accuracy 0.2 °C). Those not indicated in this section are given in Table 2. Elemental analyses were carried out by Ciba-Geigy; F-containing substances are known to give slightly too high O-contents; elements indicated as <X% are below the detection limit. ¹H-NMR were recorded on a Bruker Spectrospin 200 MHz spectrometer. Concentrations are about 0.1 M, when not specified. All dynamic viscosity measurements were carried out on the Haake microviscosimeter-VT500 viscosimeter, thermally controlled by a Haake D8 thermostat-cryostat. Conductivity measurements were performed in a two platinum electrode conductivity cell (cell constant $K_{\text{cell}} = 0.68$, determined by aqueous KCl standard solution), under thermostated bath conditions. The ac impedance technique was employed and impedance measurements taken above 1 kHz.²⁰ For the electrochemical characterization of the molten salts, a two-compartment glass cell was employed, containing about 2 mL of solution. The working and counter electrodes were constructed from Pt, a disk (0.78 mm²) sealed in Pyrex tubing and wire, respectively. The reference electrode was based on the iodide/triiodide couple. In this electrode system, the molten salt solvent being investigated in the working electrode compartment was employed in conjunction with a Pt electrode.² A solution of 15mM iodine and 60 mM of NPr_4^+I^- was made up using the molten salt under study; a fine glass frit connected the reference electrode solution to the main body of the cell. Solutions were maintained under Ar. The PC-controlled Ecochemie Model Autolab P20 potentiostat, equipped with frequency response analysis, was used for cyclic and linear sweep voltammetry, as well as for ac impedance measurements. For the photophysical probe studies, pyrene (Fluka), pyrene carboxaldehyde (Aldrich), and 1-bromonaphthalene were purified respectively by sublimation, repeated recrystallization from ethanol, and distillation under reduced pressure. Stock solutions in $\text{EtMeIm}^+\text{Tf}_2\text{N}^-$, ca. 10^{-3} M, were first prepared by dissolving appropriate quantities of the probe molecules. Solutions for emission were prepared by appropriate dilution of these stock solutions using neat $\text{EtMeIm}^+\text{Tf}_2\text{N}^-$. Steady state emission measurements were made on a SPEX fluorolog spectrofluorimeter equipped with a red-sensitive Hamamatsu R2658 photomultiplier tube. Corrected emission spectra were recorded in each case using appropriate correction files recorded earlier. The solutions were thoroughly degassed by slow bubbling of Ar for at least 15 min. prior to measurements. Emission lifetimes were made on a time-correlated single photon counting unit.

1-Ethylimidazole. In a three-necked, 500-mL round-bottomed flask equipped with reflux condenser, 100-mL dropping funnel, and magnetic stirrer, 50 g (0.734 mol) of imidazole (Fluka, *puriss. p.a.*) was diluted

(27) (a) Kalyanasundaram K.; Thomas, J. K.; Grieser, F., *Chem. Phys. Lett.* **1977**, *51*, 501–505. (b) Turro, N. J.; Liu, K. C.; Chow, M. F.; Lee, P. *Photochem. Photobiol.* **1977**, *27*, 523–529. (c) Vo-Dinh, T. *Room Temperature Phosphorimetry in Chemical Analysis*; John Wiley: New York, 1984.

under Ar in 250 mL of absolute ethanol. Then 55.0 g (0.81 mol) of sodium ethoxide (Fluka, *pract.*) was added in one portion and the resulting warm solution was stirred for 30 min. Then 88.0 g (0.81 mol) of freshly distilled bromoethane (Fluka, *purum*) was added dropwise over 1 h. The solution was then refluxed for 30 min. After cooling down to room temperature, the mixture was filtered to remove the precipitated NaBr, concentrated on a Rotavapor, refiltered to remove some more NaBr, and finally concentrated at 70 °C, under 100 mbar of pressure. The residual liquid was distilled under 12 mbar of pressure over a 10-cm Vigreux column, collecting the pure 1-ethylimidazole at 79–81 °C. Yield: 35.7 g (50%). ¹H-NMR (CDCl₃, δ/ppm relative to TMS): 7.47 (s, 1H), 6.92 (s, 1H), 3.98 (q, 2H, *J* = 9.0 Hz), 1.44 (t, 3H, *J* = 9.0 Hz).

1-Ethyl-2-methylimidazole. The same procedure was used, with 45.3 g (0.59 mol) of 2-methylimidazole (Fluka, *purum*) 44.1 g (0.65 mol) of sodium ethoxide, and 70.9 g (0.65 mol) of bromoethane in 250 mL of absolute ethanol to give a pure fraction of 20 g of product boiling at 94 °C under 11 mbar of pressure (31%). ¹H-NMR (CDCl₃, δ/ppm relative to TMS): 6.90 (s, 1H), 6.83 (s, 1H), 3.88 (q, 2H, *J* = 9.0 Hz), 2.38 (s, 3H), 1.37 (t, 3H, *J* = 9.0 Hz).

1-Ethyl-4-methylimidazole. The same procedure was used, with 12.3 g (0.150 mol) of 4-methylimidazole (Fluka, *purum*), 11.4 g (0.167 mol) of sodium ethoxide and 34.9 g (0.224 mol) of iodoethane in 100 mL of absolute ethanol to give a pure fraction of 3.2 g of product boiling at 92 °C under 11 mbar of pressure (19%). ¹H-NMR (CDCl₃, δ/ppm relative to TMS): 7.34 (s, 1H), 6.63 (s, 1H), 3.90 (q, 2H, *J* = 9.0 Hz), 2.12 (s, 3H), 1.41 (t, 3H, *J* = 9.0 Hz).

1,2-Diethylimidazole. First, 28.83 g (0.30 mol) of 2-ethylimidazole (Fluka, *purum*) was diluted in 300 mL acetonitrile (Fluka, *puriss.*). Then 21.72 g (0.32 mol) of sodium ethoxide was added, and the solution was heated under stirring for 4 h to 60 °C. A solution of 34.88 g (0.32 mol) of bromoethane in 80 mL of acetonitrile was added dropwise to the vigorously stirred solution, over 2 h. Heating was continued for 15 h. The precipitate of NaBr was filtered off and the solvent was removed on a Rotavapor. The residue was distilled through a 10 cm Vigreux column, under 12 mbar of pressure. The unique fraction was collected at 93–94 °C: yield 19.30 g (52%). ¹H-NMR (CDCl₃, δ/ppm relative to TMS): 6.94 (d, 1H, *J* = 1.5 Hz), 6.83 (d, 1H, *J* = 1.5 Hz), 3.89 (q, 2H, *J* = 9.2 Hz), 2.68 (q, 2H, *J* = 9.5 Hz), 1.42–1.30 (2 t, 6H, *J* = 9.3 Hz).

1-Ethyl-3-methylimidazolium bromide (EtMeIm⁺Br⁻). The same apparatus was used. Under vigorous stirring, 147 g (1.35 mol) of freshly distilled bromoethane was added dropwise over 1 h to a solution of 37.0 g (0.45 mol) of 1-methylimidazole (Fluka, *puriss.*) in 200 mL of 1,1,1-trichloroethane (Fluka, *puriss.*). The mixture, already turbid, was refluxed for 2 h. The molten salt was decanted from the hot solution in a separatory funnel, washed twice with 100 mL of trichloroethane, and dried on a Rotavapor for 1 h at 70 °C under 0.1 mbar of pressure: Yield: 78.1 g white solid (91%). In a scaled-up synthesis, 365.5 g of imidazole and 730 g of bromoethane in 1.5 l trichloroethane yielded 845 g of MeEtIm⁺Br⁻ (99.3%). Mp: 76.5 °C. ¹H-NMR (D₂O, δ/ppm relative to DSS): 8.74 (s, 1H), 7.51 (t, 2H, *J* = 2.2 Hz), 4.25 (q, 2H, *J* = 9.3 Hz), 3.91 (s, 3H), 1.52 (t, 3H, *J* = 9.3 Hz).

1-Butyl-3-methylimidazolium Bromide (MeEtIm⁺Br⁻). The same procedure was used as for EtMeIm⁺Br⁻. From 23.22 g (0.283 mol) of 1-methylimidazole and 39.00 g (0.285 mmol) of bromoethane, there was obtained 39.4 g of BuMeIm⁺Br⁻ (64%), as a viscous liquid. ¹H-NMR (acetone-*d*₃, δ/ppm relative to TMS): 10.17 (s, 1H), 8.10 (s, 1H), 8.01 (s, 1H), 4.50 (t, 2H, *J* = 9.3 Hz), 4.16 (s, 3H), 1.96 (m, 2H), 1.37 (m, 2H, *J* = 9.5 Hz), 0.95 (t, 3H, *J* = 9.1 Hz).

1,3-Diethylimidazolium Bromide (Et₂Im⁺Br⁻). The same procedure was used as for EtMeIm⁺Br⁻. From 33.9 g (0.353 mol) of 1-ethylimidazole and 96.7 g (0.89 mmol) of bromoethane, there was obtained 42.5 g of Et₂Im⁺Br⁻ (59%), mp 53 °C. ¹H-NMR (acetone-*d*₃, δ/ppm relative to TMS): 10.25 (s, 1H), 7.75 (t, 2H, *J* = 2.2 Hz), 4.42 (q, 4H, *J* = 9.2 Hz), 1.56 (q, 6H, *J* = 9.0 Hz).

1-Isobutyl-3-methylimidazolium Bromide (*i*-BuMeIm⁺Br⁻). The same procedure was used as for EtMeIm⁺Br⁻, except that MeOH was used as solvent as no reaction took place in trichloroethane. Reflux was maintained for 15 h. From 17.03 g (0.208 mol) of 1-methylimidazole and 28.41 g (0.208 mmol) of freshly distilled 1-bromo-2-

methylpropane (Fluka, *purum*), there was obtained 4.33 g of *i*-BuMeIm⁺Br⁻ (9.5%). ¹H-NMR (D₂O, δ/ppm relative to DSS): 8.74 (s, 1H), 7.47 (m, 2H), 4.04 (d, 2H, *J* = 9.0 Hz), 3.92 (s, 3H), 2.16 (sept, 1H, *J* = 8.5 Hz), 0.94 (d, 6H, *J* = 8.5 Hz).

1-Butyl-3-ethylimidazolium Bromide (BuEtIm⁺Br⁻). The same procedure was used as for EtMeIm⁺Br⁻. From 18.02 g (0.187 mol) of 1-ethylimidazole and 26.08 g (0.190 mmol) of freshly distilled bromobutane (Fluka, *purum*), there was obtained 39.1 g of BuEtIm⁺Br⁻ (90%), which becomes glassy upon cooling to -25 °C, without crystallization. ¹H-NMR (acetone-*d*₃, δ/ppm relative to TMS): 10.23 (s, 1H), 8.00 (s, 2H), 7.71 (t, 1H, *J* = 2.2 Hz), 4.56–4.44 (m, 4H), 1.97 (quint, 2H, *J* = 9.0 Hz), 1.60 (t, 3H, *J* = 9.0 Hz), 0.96 (t, 3H, *J* = 9.0 Hz).

1-Ethyl-2,3-dimethylimidazolium Bromide (EtMe₂Im⁺Br⁻). The same procedure was used as for EtMeIm⁺Br⁻. From 17.07 g (0.178 mol) of 1,2-dimethylimidazole (Aldrich) and 61.7 g (0.566 mmol) of bromoethane, there was obtained 17.4 g of Et₂Im⁺Br⁻ (48%) as an oil that supercools and turns glassy without crystallizing. ¹H-NMR (D₂O, δ/ppm relative to DSS): 7.36 (d, 1H, *J* = 2.7 Hz), 7.36 (d, 1H, *J* = 2.7 Hz), 4.15 (s, 2H, *J* = 9.2 Hz), 3.92 (s, 3H), 3.77 (s, 3H), 2.95 (s, 3H), 1.43 (t, 3H, *J* = 9.0 Hz).

1,3-Dimethylimidazolium Iodide (Me₂Im⁺I⁻). The same procedure was used as for EtMeIm⁺Br⁻, except that the reaction was carried out under Ar to prevent iodide oxidation. From 32.0 g (0.39 mol) of 1-methylimidazole and 55.4 g (0.39 mol) of methyl iodide, there was obtained 12.0 g Me₂Im⁺I⁻ (80%), mp 76 °C. ¹H-NMR (acetone-*d*₃, δ/ppm relative to TMS): 9.57 (s, 1H), 7.84 (d, 2H, *J* = 2.2 Hz), 4.12 (s, 6H).

1,3-Dimethylimidazolium Trifluoromethanesulfonate (Me₂Im⁺TfO⁻). The same procedure was used as for EtMeIm⁺Br⁻, except that the reaction was carried out under Ar to prevent methyl triflate hydrolysis, with 1,1,1-trichloroethane stored over molecular sieve ([H₂O] = 1.5 mM). From 4.28 g (52 mmol) of 1-methylimidazole and 8.55 g (52 mmol) of methyl triflate (Fluka, *purum*) diluted in 20 mL of 1,1,1-trichloroethane, there was obtained 12.0 g of Me₂Im⁺TfO⁻ (94%). ¹H-NMR (acetone-*d*₃, δ/ppm relative to TMS): 9.04 (s, 1H), 7.66 (d, 2H, *J* = 2.0 Hz), 4.04 (s, 6H).

1-Ethyl-3-methylimidazolium Trifluoromethanesulfonate (EtMeIm⁺TfO⁻). The same procedure was used as for Me₂Im⁺TfO⁻. From 19.2 g (0.20 mol) of 1-ethylimidazole and 32.1 g (0.196 mol) of methyl triflate, there was obtained 44.9 g of EtMeIm⁺TfO⁻ (88%). Anal. Calcd for C₇H₁₁N₂O₃F₃S: C, 32.31; H, 4.26; N, 10.76; O, 18.44; F, 21.90; S, 12.32. Found: C, 31.58/31.60; H, 4.17/4.45; N, 10.34/10.54; O, 19.2/19.3; S, 12.24. ¹H-NMR (0.188 M in acetone-*d*₃, δ/ppm relative to TMS): 9.10 (s, 1H), 7.78 (t, 1H, *J* = 2.2 Hz), 7.71 (t, 1H, *J* = 2.2 Hz), 4.39 (q, 2H, *J* = 9.3 Hz), 4.05 (s, 3H), 1.56 (t, 3H, *J* = 9.0 Hz).

1-Butyl-3-methylimidazolium Trifluoromethanesulfonate (BuMeIm⁺TfO⁻). The same procedure was used as for Me₂Im⁺TfO⁻. From 12.42 g (0.100 mol) of redistilled 1-butylimidazole (Aldrich) and 17.23 g (0.105 mol) of methyl triflate, there was obtained 26.98 g of EtMeIm⁺TfO⁻ (94%). ¹H-NMR (acetone-*d*₃, δ/ppm relative to TMS): 9.11 (s, 1H), 7.77 (t, 1H, *J* = 2.2 Hz), 7.71 (t, 1H, *J* = 2.2 Hz), 4.35 (t, 2H, *J* = 9.3 Hz), 4.04 (s, 3H), 2.00–1.90 (m, 2H), 1.38–1.29 (m, 2H), 0.87 (t, 3H, *J* = 9.2 Hz).

1-(2-Methoxyethyl)-3-methylimidazolium Trifluoromethanesulfonate (MeOEtMeIm⁺TfO⁻). The entire process was carried out under Ar. In a 250-mL three-necked flask under Ar, 6.10 g (77 mmol) of pyridine (Fluka, *puriss.*, *abs.*) was added by syringe to a strongly stirred solution of 20.4 g (72 mmol) of trifluoromethanesulfonic anhydride (Aldrich), leading to the formation of an abundant precipitate of *N*-triflylpyridinium triflate. To the cooled mixture (0 °C), was added by syringe 6.05 g (79.5 mmol) of 2-methoxyethanol (Fluka, *puriss.*, *abs.*). After 15 min at room temperature, the solution was diluted by 100 mL of pentane to ensure the complete precipitation of pyridinium triflate, filtered quickly, and concentrated to 30 mL on a 30 °C water bath, under 600 mbar of pressure. To that solution was added dropwise under stirring a solution of 5.76 g (70.2 mmol) of 1-methylimidazole in 30 mL of trichloroethane. The mixture was then refluxed for 1 h and worked up as for Me₂Im⁺TfO⁻. Yield: 14.11 g (69%). Anal. Calcd for C₈H₁₃N₂O₄F₃S: C, 33.10; H, 4.51; N, 9.65; O, 22.05; F, 19.64; S, 11.05. Found: C, 33.26/33.52; H, 4.58/4.42; N, 10.24/9.97; O, 22.5; S, 10.77. ¹H-NMR (acetone-*d*₃, δ/ppm relative to TMS): 9.05

(s, 1H), 7.73–7.68 (2 overlapping t, 2H, $J = 2.2$ Hz), 4.52 (t, 2H, $J = 5.9$ Hz), 4.06 (s, 3H), 3.80 (t, 2H, $J = 5.0$ Hz), 3.35 (s, 3H).

1-(2,2,2-Trifluoroethyl)-3-methylimidazolium Trifluoromethanesulfonate (CF₃CH₂MeIm⁺TfO⁻). The same procedure was used as for MeOEtMeIm⁺TfO⁻. From 20.4 g (72.0 mmol) of trifluoromethanesulfonic anhydride, 5.93 g (75 mmol) of pyridine, and 7.20 g (72 mmol) of 1,1,1-trifluoroethanol (Fluka, *puriss.*) there was obtained 6.20 g of CF₃CH₂MeIm⁺TfO⁻ (28%) as a light brown solid. Anal. Calcd for C₇H₈N₂O₃F₆S: C, 26.76; H, 2.57; N, 8.92; O, 15.28; F, 36.28; S, 15.28. Found: C, 27.10; H, 2.50; N, 9.15; O, 15.8; F, 36.03. ¹H-NMR (acetone-*d*₃, δ /ppm relative to TMS): 9.34 (s, 1H), 7.91 (s, 1H), 7.87 (t, 1H, $J = 2.5$ Hz), 5.40 (q, 2H, $J = 10.7$ Hz), 4.14 (s, 3H).

1,3-Diethylimidazolium Trifluoromethanesulfonate (Et₂Im⁺TfO⁻). The same procedure was used as for Me₂Im⁺TfO⁻. From 5.93 g (61.7 mmol) of 1-ethylimidazole and 10.97 g (61.7 mmol) of ethyl triflate (Fluka, *purum*), there was obtained 15.9 g of Et₂Im⁺TfO⁻ (94%). ¹H-NMR (acetone-*d*₃, δ /ppm relative to TMS): 9.17 (s, 1H), 7.78 (d, 2H, $J = 2.0$ Hz), 4.39 (q, 4H, $J = 8.8$ Hz), 1.57 (t, 6H, $J = 9.0$ Hz).

1-Ethyl-2,3-dimethylimidazolium Trifluoromethanesulfonate (1-Et-2,3-Me₂Im⁺TfO⁻). The same procedure was used as for Me₂Im⁺TfO⁻. From 5.93 g (61.7 mmol) of 1-ethylimidazole and 10.97 g (61.7 mmol) of ethyl triflate (Fluka, *purum*), there was obtained 15.9 g of Et₂Im⁺TfO⁻ (94%). ¹H-NMR (acetone-*d*₃, δ /ppm relative to TMS): 7.64 (d, 1H, $J = 2.8$ Hz), 7.59 (d, 1H, $J = 2.8$ Hz), 4.33 (q, 2H, $J = 9.3$ Hz), 3.94 (s, 2H), 2.78 (s, 3H), 1.49 (t, 3H, $J = 9.0$ Hz).

1-Ethyl-3,4-dimethylimidazolium Trifluoromethanesulfonate (1-Et-3,4-Me₂Im⁺TfO⁻). The same procedure was used as for Me₂Im⁺TfO⁻. From 2.62 g (23.8 mmol) of 1-ethyl-4-methylimidazole and 3.91 g (23.8 mmol) of methyl triflate, there was obtained 5.67 g of 1-Et-3,4-Me₂Im⁺TfO⁻ (87%). ¹H-NMR (acetone-*d*₃, δ /ppm relative to TMS): 9.01 (s, 1H), 7.52 (s, 1H), 4.30 (t, 2H, $J = 9.2$ Hz), 3.91 (s, 3H), 2.39 (s, 3H), 1.53 (t, 3H, $J = 9.0$ Hz). The product contains about 5% 1-ethyl-3,5-dimethyl isomer (see 1-Et-3,4-Me₂Im⁺Tf₂N⁻).

1,3-Diethyl-4-methylimidazolium Trifluoromethanesulfonate (1,3-Et₂-4-MeIm⁺TfO⁻). The same procedure was used as for Me₂Im⁺TfO⁻. From 4.43 g (40.2 mmol) of 1-ethyl-4-methylimidazole and 7.17 g (40.3 mmol) of ethyl triflate, there was obtained 8.83 g of 1,3-Et₂-4-MeIm⁺TfO⁻ (76%). Anal. Calcd for C₉H₁₅N₂O₄F₆S: C, 37.50; H, 5.24; N, 9.72; O, 16.65; F, 19.77; S, 11.12. Found: C, 36.70/37.03; H, 5.28/5.03; N, 9.32/9.58; O, 18.6; S, 11.35. ¹H-NMR (acetone-*d*₃, δ /ppm relative to TMS): 9.06 (d, 1H, $J = 2.0$ Hz), 7.54 (s, 1H), 4.30 (m, 2H, $J = 9.2$ and 2.5 Hz), 2.41 (s, 3H), 1.53 (t, 6H, $J = 9.0$ Hz).

1,2-Diethyl-3-methylimidazolium Trifluoromethanesulfonate (1,2-Et₂-3-MeIm⁺TfO⁻). The same procedure was used as for Me₂Im⁺TfO⁻. From 5.60 g (45.2 mmol) of 1,2-diethylimidazole and 7.40 g (45.2 mmol) of methyl triflate, there was obtained 12.38 g of 1,2-Et₂-3-MeIm⁺TfO⁻ (95%). ¹H-NMR (acetone-*d*₃, δ /ppm relative to TMS): 7.68 (d, 1H, $J = 2.5$ Hz), 7.63 (d, 1H, $J = 2.5$ Hz), 4.37 (q, 2H, $J = 9.0$ Hz), 3.24 (q, 2H, $J = 9.5$ Hz), 1.53 (t, 3H, $J = 9.0$ Hz), 1.36 (t, 3H, $J = 9.0$ Hz).

1-Ethyl-3-methylimidazolium Nonafluorobutanesulfonate (EtMeIm⁺NfO⁻). A 19.10 g (0.10 mol) sample of EtMeIm⁺Br⁻ in 50 mL of H₂O and 33.80 g (0.10 mol) of potassium nonafluorobutanesulfonate (Fluka, *purum*), in 100 mL of H₂O at 70 °C were mixed. The solution was extracted by 100 mL of CH₂Cl₂, and the extract was concentrated and dried 2 h at 60 °C under 0.1 mbar of pressure to afford 24.4 g of EtMeIm⁺NfO⁻ (59%) free of Br⁻ (no precipitate with AgNO₃). Further extractions gave a salt that produced a precipitate with AgNO₃. ¹H-NMR (0.139 M in acetone-*d*₃, δ /ppm relative to TMS): identical to EtMeIm⁺TfO⁻.

1-Butyl-3-methylimidazolium Nonafluorobutanesulfonate (BuMeIm⁺NfO⁻). A solution of 9.54 g (43.5 mmol) of BuMeIm⁺Br⁻ in 50 mL of H₂O and a solution of 14.16 g (41.9 mmol) of KNfO in 100 mL of H₂O at 70 °C were mixed under stirring. After decantation, the liquid salt was washed twice with 30 mL H₂O and dried 2 h at 150 °C under 0.1 mbar of pressure to afford 14.40 g of BuMeIm⁺NfO⁻ (78%). Anal. Calcd for C₁₂H₁₅N₂O₄F₆S: C, 32.88; H, 3.45; N, 6.39; O, 10.95; F, 39.01; S, 7.31. Found: C, 32.21/32.08; H, 3.65/3.42; N, 6.53/6.10; O, 12.1; F, 38.37. ¹H-NMR (acetone-*d*₃, δ /ppm relative to TMS): identical to BuMeIm⁺TfO⁻.

1,3-Dimethylimidazolium Bis((trifluoromethyl)sulfonyl)amide (Me₂Im⁺Tf₂N⁻). Same procedure as for EtMeIm⁺NfO⁻. From 6.02

g (27.0 mmol) of Me₂Im⁺I⁻ and 7.75 g (27.0 mmol) of lithium bis((trifluoromethyl)sulfonyl)amide (3M or Fluka, *puriss.*), there was obtained 6.08 g of Me₂Im⁺Tf₂N⁻ (60%). Anal. Calcd for C₇H₉N₃O₄F₆S₂: C, 22.29; H, 2.40; N, 11.14; O, 16.96; F, 30.21; S, 17.00. Found: C, 22.33; H, 2.30; N, 11.04; O, 17.3; S, 16.97. ¹H-NMR (acetone-*d*₃, δ /ppm relative to TMS): 8.94 (s, 1H), rest identical to Me₂Im⁺TfO⁻.

1-Ethyl-3-methylimidazolium Bis((trifluoromethyl)sulfonyl)amide (EtMeIm⁺Tf₂N⁻). The same procedure was used as for Me₂Im⁺Tf₂N⁻. From 20.54 g (107 mmol) of EtMeIm⁺Br⁻ and 30.85 g (107 mmol) of LiTf₂N, there was obtained 35.11 g of EtMeIm⁺Tf₂N⁻ (84%). Anal. Calcd for C₈H₁₁N₃O₄F₆S₂: C, 24.56; H, 2.83; N, 10.74; O, 16.35; F, 29.13; S, 16.39. Found: C, 24.38; H, 2.74; N, 10.64; O, 16.8; S, 16.75, Li, <0.1 ppm; Br <0.3%. ¹H-NMR (0.112 M in acetone-*d*₃, δ /ppm relative to TMS): 9.03 (s, 1H), rest identical to EtMeIm⁺TfO⁻.

1-Butyl-3-methylimidazolium Bis((trifluoromethyl)sulfonyl)amide (BuMeIm⁺Tf₂N⁻). The same procedure was used as for Me₂Im⁺Tf₂N⁻. From 3.18 g (14.5 mmol) of BuMeIm⁺Br⁻ and 4.14 g (14.5 mmol) of LiTf₂N, there was obtained 6.04 g of BuMeIm⁺Tf₂N⁻ (90%). ¹H-NMR (acetone-*d*₃, δ /ppm relative to TMS): 9.02 (s, 1H), 7.76 (t, 1H, $J = 2.2$ Hz), 7.71 (t, 1H, $J = 2.2$ Hz), 4.37 (t, 2H, $J = 9.3$ Hz), 4.07 (s, 3H), 2.00–1.90 (m, 2H), 1.39 (sext, 2H, $J = 9.2$ Hz), 0.95 (t, 3H, $J = 9.2$ Hz).

1-Isobutyl-3-methylimidazolium Bis((trifluoromethyl)sulfonyl)amide (*i*-BuMeIm⁺Tf₂N⁻). The same procedure was used as for Me₂Im⁺Tf₂N⁻. From 4.33 g (19.7 mmol) *iso*-BuMeIm⁺Br⁻ and 5.67 g (19.7 mmol) of LiTf₂N, there was obtained 5.16 g of *i*-BuMeIm⁺Tf₂N⁻ (62%). ¹H-NMR (acetone-*d*₃, δ /ppm relative to TMS): 9.01 (s, 1H), 7.73 (s, 2H), 4.19 (d, 2H, $J = 9.2$ Hz), 4.08 (s, 3H), 2.16 (sept, 1H, $J = 8.5$ Hz), 0.94 (d, 6H, $J = 8.5$ Hz).

1-(2-Methoxyethyl)-3-methylimidazolium Bis((trifluoromethyl)sulfonyl)amide (MeOEtMeIm⁺Tf₂N⁻). The same procedure was used as for Me₂Im⁺Tf₂N⁻. From 6.76 g (23.3 mmol) of MeOEtMeIm⁺TfO⁻ and 6.68 g (23.3 mmol) of LiTf₂N, there was obtained 6.86 g of MeOEtMeIm⁺Tf₂N⁻ (70%). Anal. Calcd for C₉H₁₃N₃O₅F₆S₂: C, 25.66; H, 3.11; N, 9.97; O, 18.99; F, 27.05; S, 15.22. Found: C, 25.70; H, 2.95; N, 9.87; O, 19.4; S, 15.03. ¹H-NMR (acetone-*d*₃, δ /ppm relative to TMS): 8.99 (s, 1H); the rest identical to those of MeOEtMeIm⁺TfO⁻.

1-(2,2,2-Trifluoroethyl)-3-methylimidazolium Bis((trifluoromethyl)sulfonyl)amide (CF₃CH₂MeIm⁺Tf₂N⁻). The same procedure was used as for Me₂Im⁺Tf₂N⁻. From 2.53 g (8.05 mmol) of CF₃CH₂MeIm⁺TfO⁻ and 2.31 g (8.05 mmol) of LiTf₂N, there was obtained 1.86 g of CF₃CH₂MeIm⁺Tf₂N⁻ (52%). ¹H-NMR (acetone-*d*₃, δ /ppm relative to TMS): 9.32 (s, 1H), 7.93 (s, 1H), 7.89 (t, 1H, $J = 2.5$ Hz), 5.43 (q, 2H, $J = 10.7$ Hz), 4.18 (s, 3H).

1,2-Diethylimidazolium Bis((trifluoromethyl)sulfonyl)amide (Et₂Im⁺Tf₂N⁻). The same procedure was used as for Me₂Im⁺Tf₂N⁻. From 8.63 g (42.1 mmol) of Et₂Im⁺Br⁻ and 12.08 g (42.1 mmol) of LiTf₂N, there was obtained 13.88 g of Et₂Im⁺Tf₂N⁻ (82%). ¹H-NMR (acetone-*d*₃, δ /ppm relative to TMS): 9.08 (s, 1H), the rest identical to those of Et₂MeIm⁺TfO⁻.

1-Butyl-3-ethylimidazolium Bis((trifluoromethyl)sulfonyl)amide (BuMeIm⁺Tf₂N⁻). The same procedure was used as for Me₂Im⁺Tf₂N⁻. From 5.35 g (22.7 mmol) of BuEtIm⁺Br⁻ and 6.52 g (22.7 mmol) of LiTf₂N, there was obtained 8.70 g of BuEtIm⁺Tf₂N⁻ (89%). ¹H-NMR (acetone-*d*₃, δ /ppm relative to TMS): 9.09 (s, 1H), 7.79 (t, 2H, $J = 2.0$ Hz), 4.47–4.33 (m, 4H), 1.94 (q, 2H, $J = 9.2$ Hz), 1.59 (t, 3H, $J = 9.0$ Hz), 1.39 (sext, 2H, $J = 9.8$ Hz), 0.95 (t, 3H, $J = 9.2$ Hz).

1-Ethyl-2,3-dimethylimidazolium Bis((trifluoromethyl)sulfonyl)amide (1-Et-2,3-Me₂Im⁺Tf₂N⁻). The same procedure was used as for Me₂Im⁺Tf₂N⁻. From 4.31 g (21.0 mmol) of 1-Et-2,3-Me₂Im⁺Br⁻ and 6.04 g (21.0 mmol) of LiTf₂N, there was obtained 6.52 g of EtMe₂Im⁺Tf₂N⁻ (77%). Anal. Calcd for C₉H₁₃N₃O₄F₆S₂: C, 26.67; H, 3.23; N, 10.37; O, 15.79; F, 28.12; S, 15.82. Found: C, 26.40; H, 3.01; N, 10.08; O, 16.2; S, 15.55. ¹H-NMR (acetone-*d*₃, δ /ppm relative to TMS): 7.61 (d, 1H, $J = 2.8$ Hz), 7.56 (d, 1H, $J = 2.8$ Hz), 4.32 (q, 2H, $J = 9.2$ Hz), 3.49 (s, 3H), 2.78 (s, 3H), 1.49 (t, 3H, $J = 9.2$ Hz).

1-Ethyl-3,4-dimethylimidazolium Bis((trifluoromethyl)sulfonyl)amide (1-Et-3,4-Me₂Im⁺Tf₂N⁻). The same procedure was used as for Me₂Im⁺Tf₂N⁻. From 6.54 g (22.7 mmol) of 1-Et-3,4-Me₂Im⁺TfO⁻ and 6.51 g (22.7 mmol) of LiTf₂N, there was obtained 7.48 g of

EtMe₂Im⁺Tf₂N⁻ (79%). Anal. Calcd for C₉H₁₃N₃O₄F₆S₂: C, 26.67; H, 3.23; N, 10.37; O, 15.79; F, 28.12; S, 15.82. Found: C, 26.39; H, 3.10; N, 10.18; O, 16.3; S, 15.66. ¹H-NMR (acetone-*d*₃, δ/ppm relative to TMS): 9.2% 1-Et-3,4-Me₂Im⁺Tf₂N⁻, 8.92 (s, 1H), 7.51 (s, 1H), 4.32 (q, 2H, *J* = 9.3 Hz), 3.93 (s, 3H), 2.41 (d, 3H, *J* = 1.4 Hz), 1.54 (t, 3H, *J* = 9.0 Hz); 8% 1-Et-3,5-Me₂Im⁺Tf₂N⁻, 8.92 (s, 1H), 7.44 (s, 1H), 4.32 (q, 2H, *J* = 9.3 Hz), 3.99 (s, 3H), 2.43 (d, 3H, *J* = 1.4 Hz), 1.54 (t, 3H, *J* = 9.0 Hz).

1,3-Diethyl-4-methylimidazolium Bis((trifluoromethyl)sulfonyl)-amide (1,3-Et₂-4-MeIm⁺Tf₂N⁻). The same procedure was used as for Me₂Im⁺Tf₂N⁻. From 2.38 g (8.68 mmol) of 1,3-Et₂-4-MeIm⁺TfO⁻ and 2.49 g (8.68 mmol) of LiTf₂N, there was obtained 3.52 g of Et₂MeIm⁺Tf₂N⁻ (67%). ¹H-NMR (acetone-*d*₃, δ/ppm relative to TMS): 8.96 (d, 1H, *J* = 1.5 Hz), 7.51 (s, 1H), 4.30 (m, 2H, *J* = 9.2 and 2.5 Hz), 2.43 (d, 3H, *J* = 1.5 Hz), 1.55 (t, 6H, *J* = 9.0 Hz).

1,3-Dimethylimidazolium Trifluoroacetate (1,3-Me₂Im⁺TA⁻). A 5.079 g (22.67 mmol) sample of 1,3-Me₂Im⁺I⁻ and 5.007 g (22.67 mmol) of silver trifluoroacetate (Fluka, *prurum*) were diluted in 50 mL of water each and mixed. After 1 h of stirring at 70 °C, the silver iodide was filtered off and the solution, concentrated under 12 mbar of pressure. The salt was dried 2 h at 50 °C under 0.1 mbar of pressure. Yield: 4.70 g (98.7%). ¹H-NMR (acetone-*d*₃, δ/ppm relative to TMS): 9.78 (s, 1H), 7.75 (d, 2H, *J* = 2.0 Hz), 4.06 (s, 6H).

1-Ethyl-3-methylimidazolium Trifluoroacetate (EtMeIm⁺TA⁻). The same procedure was used as for 1,3-Me₂Im⁺TA⁻. From 4.342 g (22.72 mmol) of EtMeIm⁺Br⁻ and 5.019 g (22.72 mmol) of AgTA⁻, there was obtained 4.92 g of EtMeIm⁺TA⁻ (96.6%). Anal. Calcd for C₈H₁₁N₂O₂F₃S: C, 42.86; H, 4.95; N, 12.50; O, 14.27; F, 25.42. Found: C, 41.96/41.99; H, 5.02/4.95; N, 12.21/12.19; O, 16.2; F, 24.77; Ag, 0.25%; Br, <0.3%. ¹H-NMR (0.104 M in acetone-*d*₃, δ/ppm relative to TMS): 9.92 (s, 1H), 7.86 (t, 1H, *J* = 2.2 Hz), 7.78 (t, 1H, *J* = 2.2 Hz); the rest identical to those of EtMeIm⁺TfO⁻.

Alternative procedure: 26.15 g (0.272 mol) of 1-ethylimidazole was diluted in 120 mL 1,1,1-trichloroethane. Then 69.7 g (0.544 mol) of methyl trifluoroacetate was added in one portion, and the mixture was refluxed. A turbidity appeared after a few hours. Reflux was continued for 3 days, and the molten salt was decanted, washed twice with 50 mL of trichloroethane and once with 50 mL of *tert*-butyl methyl ether, and dried for 4 h at 80 °C under 0.1 mbar of pressure to afford 59.00 g of EtMeIm⁺TA⁻ (97%).

1-Butyl-3-methylimidazolium Trifluoroacetate (BuMeIm⁺TA⁻). The same procedure was used as for 1,3-Me₂Im⁺TA⁻. From 5.089 g (23.22 mmol) of BuMeIm⁺Br⁻ and 5.089 g (23.03 mmol) of AgTA⁻, there was obtained 4.19 g of BuMeIm⁺TA⁻ (97%). ¹H-NMR (acetone-*d*₃, δ/ppm relative to TMS): 9.88 (s, 1H), 7.84 (t, 1H, *J* = 2.2 Hz), 7.78 (t, 1H, *J* = 2.2 Hz), 4.37 (t, 2H, *J* = 9.2 Hz), 4.07 (s, 3H), 1.92 (quint, 2H, *J* = 9.3 Hz), 1.37 (sext, 2H, *J* = 9.3 Hz), 0.94 (t, 3H, *J* = 9.3 Hz).

1,3-Diethylimidazolium Trifluoroacetate (1,3-Et₂Im⁺TA⁻). The same procedure was used as for 1,3-Me₂Im⁺TA⁻. From 4.683 g (22.83 mmol) of Et₂Im⁺Br⁻ and 5.043 g (22.83 mmol) of AgTA⁻, there was obtained 5.40 g of Et₂Im⁺TA⁻ (99%). ¹H-NMR (acetone-*d*₃, δ/ppm relative to TMS): 9.97 (s, 1H), 7.85 (t, 2H, *J* = 2.0 Hz), 4.42 (q, 4H, *J* = 9.2 Hz), 1.56 (q, 6H, *J* = 9.0 Hz).

1-Butyl-3-ethylimidazolium Trifluoroacetate (BuEtIm⁺TA⁻). Same procedure as for 1,3-Me₂Im⁺TA⁻. From 5.382 g (23.08 mmol) of BuEtIm⁺Br⁻ and 5.099 g (23.08 mmol) of AgTA⁻, there was obtained 6.11 g of BuEtIm⁺TA⁻ (99.4%). ¹H-NMR (acetone-*d*₃, δ/ppm relative to TMS): 10.00 (s, 1H), 7.86 (t, 2H, *J* = 3.0 Hz), 4.48–4.35 (m, 4H), 1.92 (quint, 2H, *J* = 9.2 Hz), 1.56 (t, 3H, *J* = 9.2 Hz), 1.37 (sext, 2H, *J* = 9.5 Hz), 0.94 (t, 3H, *J* = 9.0 Hz).

1-Ethyl-2,3-dimethylimidazolium Trifluoroacetate (1-Et-2,3-Me₂Im⁺TA⁻). A 5.50 g sample of 1-ethyl-2-methylimidazole (50 mmol) and 12.80 g (100 mmol) of methyl trifluoroacetate were diluted in 50 mL 1,1,1-trichloroethane. The solution was refluxed for 6 h and the salt decanted, washed twice with 20 mL of hot trichloroethane, and dried for 2 h at 60 °C under 0.1 mbar of pressure to afford 5.18 g (44%) of 1-Et-2,3-Me₂Im⁺TA⁻. ¹H-NMR (acetone-*d*₃, δ/ppm relative to TMS): 7.78 (d, 1H, *J* = 2.5 Hz), 7.74 (d, 1H, *J* = 2.5 Hz), 4.36 (q, 2H, *J* = 9.2 Hz), 3.97 (s, 3H), 2.80 (s, 3H), 1.47 (t, 3H, *J* = 9.5 Hz).

1-Ethyl-3-methylimidazolium Heptafluorobutanoate (EtMeIm⁺HB⁻). The same procedure was used as for 1,3-Me₂Im⁺TA⁻. From 3.84 g (20.1 mmol) of EtMeIm⁺Br⁻ and 6.42 g (20.0 mmol) of AgHB⁻, there was obtained 6.40 g of EtMeIm⁺HB⁻ (99.4%). ¹H-NMR (acetone-*d*₃, δ/ppm relative to TMS): 9.86 (s, 1H), 7.84 (t, 1H, *J* = 2.2 Hz), 7.76 (t, 1H, *J* = 2.2 Hz); the rest identical to those of EtMeIm⁺TA⁻.

1-Butyl-3-methylimidazolium Heptafluorobutanoate (BuMeIm⁺HB⁻). The same procedure used as for EtMeIm⁺HB⁻. From 6.670 g (30.4 mmol) of BuEtIm⁺Br⁻ and 9.678 g (30.2 mmol) of AgHB⁻, there was obtained 10.40 g of BuMeIm⁺HB⁻ (97.7%). Anal. Calcd for C₁₂H₁₅N₂O₂F₇: C, 40.92; H, 4.29; N, 7.95; O, 9.08; F, 37.75. Found: C, 40.36; H, 4.15; N, 7.89; O, 10.8; F, 35.77; Ag⁺ 7.0 ppm. ¹H-NMR (acetone-*d*₃, δ/ppm relative to TMS): 9.83 (s, 1H), 7.80 (t, 1H, *J* = 1.6 Hz), 7.75 (t, 1H, *J* = 1.6 Hz); the rest identical to those of BuMeIm⁺TA⁻.

Acknowledgment. Financial support for this work by the Swiss *Commission pour l'encouragement de la recherche scientifique* is gratefully acknowledged by the authors. We also wish to thank Dr. Christophe Barbé for thermogravimetric measurements and Dr. Lorenz Walder for fruitful discussions.

IC951325X